**RESEARCH ARTICLE**

# Design of Thermal System Integrating Chaotic Optimization Strategy and Resilient Back Propagation

**JIN QU[1] AND ZHILIN LI[2]**
[1]Spic Guizhou Jinyuan Company Ltd., Guiyang 550002, China
[2]Spic Guizhou Jinyuan Chayuan Power Company Ltd., Bijie 551800, China

Corresponding author: Zhilin Li (lzlzhm@163.com)

**ABSTRACT** With the continuous progress of technology, the equipment and technical complexity of thermal systems are increasing, resulting in higher requirements for thermal inspection systems. Traditional inspection systems often have problems such as un-reasonable path planning and incomplete equipment monitoring, which may lead to low equipment operation efficiency and even lead to safety accidents. To address these issues, this study proposed using chaotic optimization algorithms to optimize Proportion-integral-derivative (PID) controllers and using Resilient Back Propagation (RPROP) to optimize image denoising models. Subsequently, a new thermal inspection system was constructed based on improved PID controllers and optimized image denoising models. In this study, the thermal system data in the public database and the problem data set collected in the actual thermal environment were used for experimental verification. Through comparative experiments of denoising models, the improved image denoising model had a CPU running time of 0.35 s, 0.78 s, and 0.69 s for Parrot, Phantom, and Frame denoising, respectively, which was superior to the comparison models. Later, in the comparison experiment of improving the PID controller, the adjustment time, peak time, and rise time of the chaos optimized PID controller were 0.719 s, 0.731 s, and 0.595 s, respectively, which were superior to the comparative controller. Finally, an empirical analysis was conducted on the proposed new thermal inspection system. The average detection accuracy and average detection time of the new thermal inspection system were 94.6% and 28.4 minutes, respectively, which were significantly better than traditional thermal inspection systems. The above results indicate that the proposed new thermal inspection system has good performance and can be applied to the actual inspection process of thermal equipment, thereby promoting the development of the thermal systems.

**INDEX TERMS** Chaos optimization, RPROP, thermal system, image denoising, PID controller.

## I. INTRODUCTION

Thermal systems are an important research object in engineering, involving multiple physical processes such as energy conversion, heat conduction, and fluid flow [1], [2]. Thermal inspection is a component of the thermal system used for inspecting and monitoring thermal equipment. As an important tool to ensure the normal operation of equipment and prevent potential risks, the design optimization of the thermal inspection system is gradually receiving wide-

The associate editor coordinating the review of this manuscript and approving it for publication was Yang Tang.

spread attention [3], [4]. The thermal inspection system is a comprehensive system that integrates sensor monitoring, data processing, user inter-action, communication transmission, and alarm linkage to ensure the safe, efficient, and stable operation of the heating system. Thermal inspection systems also face many challenges in practical application. First of all, the traditional thermal inspection systems may have problems such as un-reasonable inspection path planning and inaccurate data collection, resulting in failure to fully and effectively monitor and evaluate the equipment. Secondly, as the size and complexity of thermal inspection systems increase, the performance and stability of the thermal

inspection system are also put forward higher requirements. Moreover, due to the complexity and variability of the thermal environment, how to achieve real-time and accurate monitoring of the equipment is also a problem that needs to be solved. To improve the efficiency and performance of thermal inspection systems, relevant experts have continuously explored new optimization methods and algorithms in recent years. Chaos Optimization Algorithm (COA) and Resilient Back Propagation (RPROP) are two methods widely used in optimization problem in recent years, and they have achieved significant results in different fields [5]. COA is a global optimization algorithm based on chaos theory, whose basic principle is to search for the optimal solution by introducing chaotic sequences [6]. Chaotic sequences have the characteristics of irregularity and strong randomness, which can effectively avoid falling into local optimal solutions [7]. In the optimization of thermal inspection systems, COA can be applied to parameter optimization, structural optimization, and other problems. The optimal solution of the system is ultimately found by continuously updating parameter values. However, COA has certain shortcomings in terms of convergence speed and search ability, so further improvement and optimization are needed [8]. RPROP is an optimization algorithm based on neural networks, whose basic idea is to achieve information transmission and update by simulating the working mode of neurons [9]. In thermal system optimization, RPROP can continuously adjust the weights and biases of neural networks to ultimately achieve system optimization [10]. This study innovatively proposes a new optimization strategy to better solve the problems existing in the practical application of the thermal inspection system, which further improves the overall performance of the thermal inspection system by integrating COA and RPROP. Through exploration and practice, it is hoped to provide a new approach and method for improving the performance of thermal systems and bring new breakthroughs and progress to research and practice in the engineering field.

This paper will be discussed in four sections. The first section is devoted to the analysis of COA, RPROP, and related studies of thermal systems. The second part describes the design of thermal inspection system which combines COA and RPROP. In the third section, the performance of the proposed thermal inspection system is analyzed using thermal system data from public databases and problem datasets collected in real thermal environments. In the fourth part, the results of the thermal inspection system proposed in the research are compared and analyzed, and the conclusion is drawn.

## II. RELATED WORKS
COA is an optimization algorithm based on chaos theory. Its basic idea is to utilize the characteristics of chaotic systems and search for the optimal solution by introducing randomness and non-linear factors. Many scholars have conducted extensive research on it. For example, Duan et al.

used COA to optimize the weight parameters and acceleration coefficients of particle swarm optimization algorithm to improve its practical application performance and introduced control factors based on chaos theory to obtain a new hybrid algorithm. Actual performance tests had confirmed that the stability, convergence speed, and accuracy of this algorithm were superior to the comparison algorithm, and its practicality was robust [11]. Premkumar et al. proposed an optimization algorithm that combined COA and gradient optimizer to address the low efficiency of photo-voltaic system efficiency estimation models. Performance testing had confirmed that the average RMSE and runtime of the optimization algorithm were 0.00237 and 18.44 seconds, which were superior to the comparison algorithm [12]. In addition, RPROP, as an improvement of back propagation algorithm, was also being studied by more and more scholars. Priyadarshi et al. proposed a fusion algorithm based on RPROP and constant modulus algorithm to improve the performance of un-supervised weight adaptive techniques used in channel equalization, and the actual performance of the fusion algorithm was tested. These results confirmed that compared to traditional algorithms, the convergence, complexity, and residual ISI of this proposed fusion algorithm had been significantly improved [13]. Abdulkarim et al. used RPROP to optimize the particle swarm optimization algorithm and obtain a hybrid method to better predict neural network time series in different environments, and comparison experimental analysis was conducted on this hybrid algorithm. These results confirmed that it a prediction accuracy of 94.7% for time series, which was significantly better than the improved algorithm [14].

A thermal system is composed of various thermal equipment and pipe-lines, used to achieve the transfer and conversion of heat energy. As the thermal system rapidly develops, there is also increasing research on it. For example, Wang et al. proposed a hierarchical deep domain adaptive thermal system to address the low accuracy of fault diagnosis in peak shaving power plants under different operating conditions. Compared to before, the fault diagnosis accuracy of this thermal system had been significantly improved under different working conditions, which had practical value [15]. Violante et al. proposed a thermal management system model that integrated thermal resources such as co-generation units, heat pumps, and boilers to better manage energy in the power grid. These performance tests confirmed that the thermal management system model could effectively manage the energy of the power grid, with significant economic benefits [16]. Toth et al. proposed a solar thermal control system based on C language and Simulink model to address the low control effectiveness of current solar thermal systems. These results confirmed that the thermal system could effectively control solar energy and had strong adaptability [17]. Babu et al. proposed a two-stage controller based on a cascaded combination of fractional order proportional derivative and proportional integral derivative to improve the performance of actual dish Stirling solar thermal systems under de-regulation. And they

used group search algorithm to optimize the controller and finally applied it to the solar thermal system. These performance tests confirmed that the dynamic response of the optimized solar thermal energy system was lower than that before optimization, resulting in a significant improvement in performance [18].

The above related research indicates that the application range of COA and RPROP is relatively wide, and there are various methods for applying them in thermal systems. However, there is currently relatively little research on combining COA and RPROP with thermal systems. To fill the research gap in this area and better improve the overall performance of thermal systems, this study combines COA and RPROP and applies them to thermal systems. In the above studies, the relative effect of the new thermal system proposed by Wang et al. was good, and its recognition accuracy was 91.2%, which could be further improved. Toth et al. proposed a solar thermal control system based on C language and simulink model. Although the adaptability was strong, its recognition performance needed to be improved. Although the dynamic response of the thermal system based on the cascade combination of fractional proportional derivative and proportional integral derivative proposed by Babu was greatly improved, its overall performance still needed to be optimized. Therefore, this study combines COA and RPROP and applies them to the thermal system to improve its overall performance and make up for the gaps in the combination of COA and RPROP with the thermal system. It is expected that the working performance of thermal engineering system can be improved in this way, so as to promote the development of the thermal engineering field.

## III. DESIGN OF THERMAL INSPECTION SYSTEM INTEGRATING COA AND IMPROVED IMAGE DENOISING MODE

Thermal inspection systems play a crucial role in ensuring the efficient and safe operation of thermal systems. So this study focuses on these systems. They can monitor and inspect thermal equipment, which is essential to prevent potential risks and maintain optimal system performance. To optimize the performance of the thermal inspection system for visible light images, a fusion RPROP image denoising model and a COA-based Proportion-integral-derivative (PID) controller are proposed in this chapter. Subsequently, a new thermal system is constructed based on the proposed denoising model and improved PID controller. This chapter mainly introduces the construction of image denoising models, optimization of PID controllers, and the architecture of new thermal systems.

### A. OPTIMIZATION OF IMAGE DENOISING MODEL WITH RPROP FUSION

The thermal inspection system for visible light images requires image denoising operations to improve image quality and signal-to-noise ratio. The purpose of denoising is to reduce or eliminate noise in images and improve the clarity and readability of images, thus better analyzing and monitor-
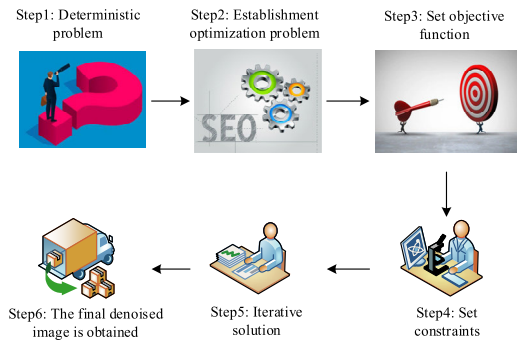


**FIGURE 1. Schematic diagram of TV in denoising.**

ing thermal equipment [19], [20]. Statistical filters, wavelet denoising, and image enhancement algorithms are common denoising methods, but they may introduce image blur, detail loss, artifacts, or noise. Total Variation (TV) is a mathematical model used to describe the dynamic behavior of a system, which has the advantages of preserving edges and details, removing noise and artifacts, and adapting to different types of noise [21]. TV reduces noise in the image by constraining TV and tries to maintain the detailed structure of the original image as much as possible. It has certain adaptability to Gaussian noise, salt and pepper noise, and other non-linear noise. Figure 1 shows the schematic diagram of TV in denoising.

From Figure 1, it should first determine the image that needs to be denoised, and then establish an optimization problem based on the principle of TV. Afterwards, in the established optimization, the total change is taken as the objective function and a difference term is added as a constraint condition. Afterwards, an iterative algorithm is used to solve the above optimization problem. In the iteration, the calculation is repeated and the image is updated until the convergence condition is reached. Finally, through multiple iterations, the optimization algorithm will gradually reduce the total change in the image and obtain a denoised image as the final result. TV is used for image denoising, but its calculation is complex and may lead to image smoothing. RPROP is an optimization method that optimizes TV image denoising by adaptively adjusting the gradient step size. RPROP monitors the gradient direction and changes of each parameter to determine the update direction and step size of the parameters in each iteration, thereby more efficiently searching the parameter space and finding better solutions. Equation (1) describes the additive noise.

$$f(x, y) = u(x, y) + n(x, y) \tag{1}$$

In equation (1), $f$ represents the observed noisy image. $n$ is a random noise with a mean of 0 and a variance of $\sigma^2$. $u$ represents the original image that needs to be solved. For the original image $u$, the equation needs to be transformed into TV and described by equation (2).

$$E = \inf_{u \in H^1(\Omega)} (\|f - u\|_{L^2(\Omega)}^2 + \lambda \|u\|_1^2) \tag{2}$$
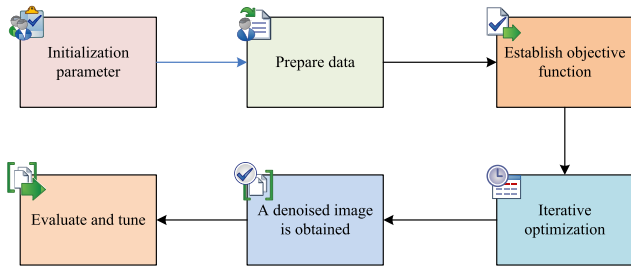
**FIGURE 2.** Image denoising of fusion RPROP.



**FIGURE 3.** Schematic diagram of PID controller.

In equation (2), $E$ is the error function. $u$ is the perturbation function. equation (2) is discretized using a finite difference scheme, resulting in equation (3).

$$\frac{\partial E^n}{\partial u_{ij}} = (f_{i,j} - u_{i,j}^n) + \lambda(\left| u_{i+1,j}^n - u_{i,j}^n \right| + \left| u_{i,j+1}^n - u_{i,j}^n \right|) \quad (3)$$

In equation (3), $i$ and $j$ both represent the scale of the iteration. $\lambda$ is a constant greater than 0. RPROP can intelligently adjust the direction and amplitude of update values based on the derivative of each parameter, making the updates of each parameter in-dependent and without mutual influence. Specifically, when the derivative of parameter is positive, RPROP will cause the updated value to decrease relative to its original value. When the derivative of parameter is negative, the updated value will increase relative to the original value. This study considers that the step size adjustment in RPROP needs to be determined based on the gradient direction of the current parameter and the direction of the previous update to determine whether back-tracking is necessary. Therefore, for two adjacent iterative updates, equation (4) describes the sign change of the error function on its derivative.

$$\Delta_i(t) = -\frac{\eta_i(t)}{\sigma_i(t)} \frac{\partial E}{\partial w_i} \quad (4)$$

In equation (4), $\Delta_i(t)$ is the update amount of the $i$th parameter at the $t$th iteration, $\eta_i(t)$ is the learning rate, $\sigma_i(t)$ is the gradient symbol, and $\frac{\partial E}{\partial w_i}$ is the partial derivative of the error function with respect to the $i$th parameter. To ensure the effectiveness of the descent, the original descent scale can be multiplied by a number less than 1 to limit the magnitude of the descent. Meanwhile, if the sign of the derivative remains un-changed, the descent scale can be multiplied by a number greater than 1 to accelerate the algorithm's convergence to the minimum point. By adopting this strategy, the downscale can be effectively adjusted, resulting in faster finding of the minimum point of the error function and improving the convergence speed and performance of the algorithm. Figure 2 shows the image denoising using RPROP fusion.

In Figure 2, in the denoising of fused RPROP images, it is first necessary to initialize the parameters required for RPROP. These parameters include step size and update rules. Next, the experiment converts the image into a matrix or vector and performs data normalization or pre-processing according to the needs of RPROP. Afterwards, based on TV,
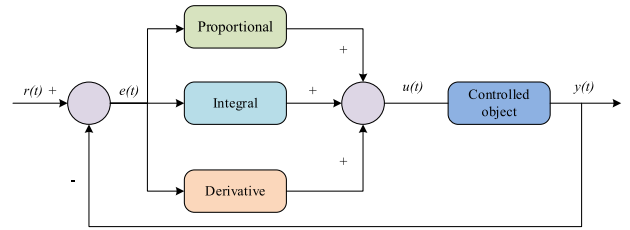
with the goal of minimizing image noise or error, RPROP is used for iterative optimization. Based on the objective function and initial parameters, the gradients of parameters are calculated, and the parameters are updated according to the step size adjustment rules of RPROP. This process is repeated until convergence or reaching the preset stop condition. Finally, in the iterative optimization, the updated parameters are used to generate denoised images.

## B. OPTIMIZATION OF CONTROLLER PARAMETERS FOR INTEGRATING COA

PID, as a commonly used closed-loop controller, can be used to stabilize control and regulate the output of the system to the desired target [22]. In the thermal inspection system, the parameter optimization of PID control can help the system quickly stabilize in the required state, which is crucial for the thermal system. Because rapid stabilization can reduce energy consumption and improve production efficiency. In addition, the system can be made more stable by optimizing the PID parameters. Integral control eliminates the steady-state error of the system by continuously adjusting the output signal, while differential control can predict its future change trend, thereby reducing the oscillation of the system. This stabilization is essential to prevent equipment damage, reduce maintenance costs, and increase production efficiency. The design of a PID controller relies on three parameters: proportional gain, integral time, and differential time, which can be adjusted to optimize the performance and stability of the control system [23]. Figure 3 shows the schematic diagram of the PID controller.

$r(t)$ in Figure 3 is the given value. $y(t)$ is the actual output value. $e(t)$ represents the control deviation, and equation (5) is the expression between them [24].

$$e(t) = r(t) - y(t) \quad (5)$$

In equation (6), $u(t)$ represents the PID control law in Figure 3 [25].

$$u(t) = K_p\left(e(t) + \frac{1}{T_i}\int_0^t e(t)dt + \frac{T_d de(t)}{dt}\right) \quad (6)$$

In the thermal inspection system of visible light images, the response and sensitivity of the image processing algorithm are adjusted through PID controller parameters. But the performance of PID controllers largely depends on the precise adjustment of parameters [26], [27]. When applying PID

controllers, it is necessary to adjust and optimize parameters based on specific system characteristics and requirements. Gradient descent and chaos algorithm are two optimization methods. Gradient descent has problems with local optimal solutions, convergence speed, and stability, while chaos algorithm has global search ability and can handle non-linear, non-convex, and high-dimensional parameter spaces. Based on these advantages, this study adopts the logistic mapping in chaos algorithm to generate chaotic sequences and optimize PID control parameters. For optimizing search, the ergodicity of chaotic motion is crucial. By traversing all states, it can find the optimal solution globally and avoid falling into local optima. In addition, the non-repetitive nature of chaotic motion can also ensure the efficiency of the optimization process. Equation (7) describes the logistic mapping [28].

$$x_{n+1} = f(x_n, \mu) = \mu x_n (1 - x_n) \tag{7}$$

In equation (7), $x_{n+1}$ is the chaotic variable, $n = 1, 2, \ldots, N$. $x_0$ is within $(0, 1)$. When $\mu$ is set to 4, the model is in a chaotic state. Equation (8) describes the assignment equation that can obtain several chaotic variables from several initial values with a difference of one bit.

$$x_{n+1} = \mu x_n (1 - x_n) \tag{8}$$

The optimization of setting a class of continuous objects for each initial variable is described by equation (9).

$$\min J(x_i), \quad i = 1, 2, \ldots, n, \quad a_i \leq x_i \leq b_i \tag{9}$$

In equation (9), $J$ is the performance indicator that reflects the dynamic and steady-state performance of the system. Equation (10) describes it.

$$J = w_1 \int_0^1 t\, |e(t)| \frac{dt}{\max(e(t))} + w_2 \sigma \tag{10}$$

In equation (10), the sum of weights $w_1$ and $w_2$ remains constant as 1. $\sigma$ is the overshoot. Equation (11) describes the discretization results of performance indicators.

$$J = \min \left[ w_1 \sum_{k=0}^{l} |e(k)| \frac{k}{\max(e(k))} + w_2 \sigma \right] \tag{11}$$

In equation (11), $l$ is the step size for each chaotic optimization. Figure 4 shows the tuning steps for Logistic mapping to optimize PID controller parameters.

According to Figure 4, optimizing PID controller parameters using Logistic mapping mainly involves seven steps. Firstly, it is necessary to determine the parameter range of the PID controller, including the range of proportional gain, integration time, and differentiation time. The second step is to initialize the parameters of the PID controller. Then there are parameters for initializing the Logistic mapping, including mapping constants and initial values. The next step is to optimize through iteration, using logistic mapping to adjust the parameters of the PID controller. In each iteration, the current PID parameters are used to control the system's state, followed by the use of logistic mapping to generate
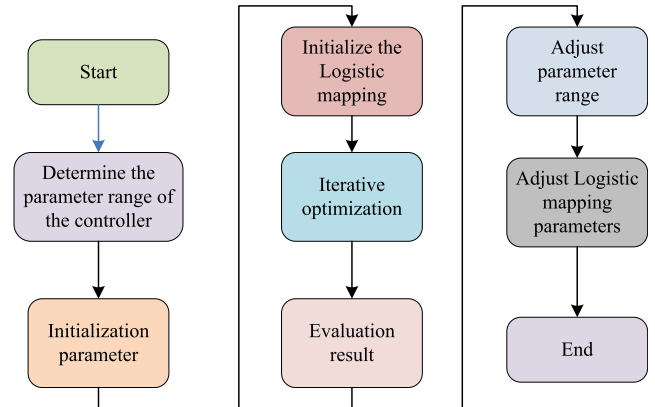


**FIGURE 4.** Tuning steps of PID controller parameters optimized by Logistic mapping.

new parameters. The new parameters are used to control the system's state. This process will be repeated multiple times until the optimal PID parameters are found. The fifth step is to evaluate the optimization results, including the performance and stability of the system. If the results are satisfactory, the optimized PID parameters can be used to control the system. If the optimization results are not satisfactory, the parameter range of the PID controller can be adjusted and the optimization can be carried out again. Finally, if the optimization results are not satisfactory after adjusting the parameter range of the PID controller, the parameters of the logistic mapping can also be adjusted and re-optimized.

### C. ESTABLISHMENT OF A THERMAL SYSTEM MODEL THAT INTEGRATES CHAOTIC OPTIMIZATION STRATEGY AND RPROP

The thermal inspection of visible light images is a system that utilizes visible light images for thermal equipment inspection. It uses visible light camera technology to obtain visible light images of thermal equipment, analyze the thermal information, and achieve monitoring of equipment operation status and anomaly detection [29]. This system can obtain real-time thermal information of equipment, identify problems such as temperature anomalies, hot spots, and leakage, and provide corresponding alarm and diagnostic results. Through this system, the inspection efficiency can be improved, the safety risks for inspection personnel can be reduced, and the potential faults and accidents can be detected and prevented in advance. In the construction of a thermal inspection system based on visible light images, this study includes a PID controller fused with COA and an image denoising TV fused with RPROP. Figure 5 shows the architecture of the constructed thermal inspection system.

According to Figure 5, the thermal inspection system architecture studied and constructed mainly includes seven modules. Firstly, it is data collection, responsible for collecting real-time data of thermal systems. The second one is image denoising, in which RPROP fusion image denoising TV is applied. By denoising the collected image data, the
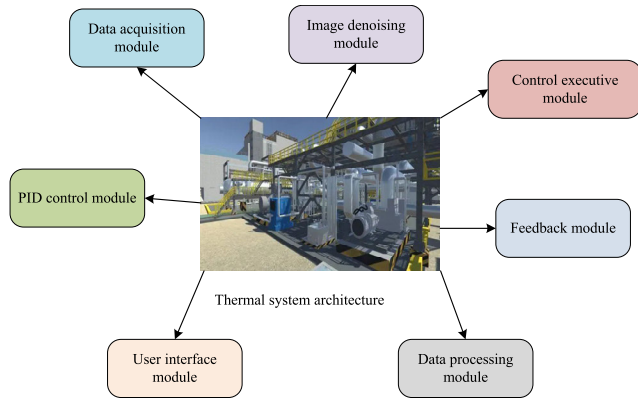
**FIGURE 5.** Thermal system architecture constructed by this research.
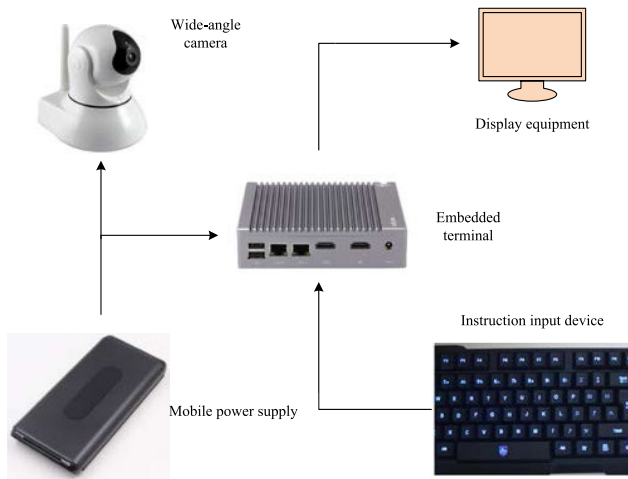


**FIGURE 6.** Mobile video capture system.

quality and accuracy of the image are improved. The PID control module mainly uses PID controller optimized by the chaotic algorithm to calculate the output signal of the collected data to control the operating status of the thermal system. The control execution module is mainly responsible for converting the output signal of PID controller into actual control actions. The functions of the feedback and data processing modules are to provide feedback on the actual operating status of the thermal system to the PID controller, and to process and analyze the collected data to provide decision support and optimize control strategies. The last module is the user interface module, which is responsible for providing a user interaction interface, allowing users to easily view the operating status and control parameters of the thermal system. In the data acquisition, it is very important to choose a correct camera to better collect real-time data of geothermal engineering systems. A mobile video capture system is used in this study to ensure complete image capture of the switch. In Figure 6, the system includes components such as a wide-angle camera, embedded terminal, mobile power supply, display, and command input device.

According to Figure 6, the video capture system of the switch achieves video data collection and monitoring by using devices such as mobile cameras and embedded terminals. And mobile power supplies provide power support for the system. Equation (12) is the power supply for mobile power sources.

$$P = V*I \tag{12}$$

In equation (12), $P$ represents the power supply. $V$ represents the voltage. $I$ represents the current. The display and instruction input devices are used to operate and display the collected video data. Equation (13) is the expression for video data acquisition and monitoring.

$$Q = f*t \tag{13}$$

In equation (13), $Q$ represents the amount of data collected and monitored. $f$ represents the frequency of data collection and monitoring. $t$ represents the time.

To maintain the stable operation of the system, the mobile power supply provides a reliable power supply for the entire system, ensuring the continuous operation of video capture. The monitor can display the captured video images in real-time, and the instruction input device is used to operate the system, control the movement of the camera, and operate other system functions. After data collection, the image denoising TV fused with RPROP is applied to denoise visible light images to improve image quality and thermal information accuracy. And thermal information is extracted from visible light images. Afterwards, a PID controller integrated with COA is applied to analyze and process the extracted thermal information, identify problems such as temperature anomalies, hot spots, and leakage, and provide corresponding alarm and diagnostic results.

## IV. COMPARATIVE ANALYSIS OF DENOISING MODELS AND CONTROL STRATEGIES AND EMPIRICAL ANALYSIS OF THERMAL SYSTEMS

The effectiveness and superiority of the proposed image denoising model, COA-based PID controller, and thermal inspection system were analyzed. Firstly, comparative experiments were conducted on the performance of image denoising models based on RPROP, and then the superiority of the PID controller fused with COA was demonstrated through comparative analysis. Finally, the effectiveness of the proposed new thermal inspection system was verified through empirical analysis.

### A. PERFORMANCE COMPARISON OF IMAGE DENOISING MODELS BASED ON RPROP

This study optimized the TV image denoising model through RPROP and obtained the RPP-TV image denoising model. To test the specific performance of this denoising model, comparative experiments were conducted with ROF, VETV, HOTV, TGV, and ATVF models. The performance of six models for denoising Parrot, Phantom, and Frame images was compared, with indicators such as CPU runtime, SNR, and
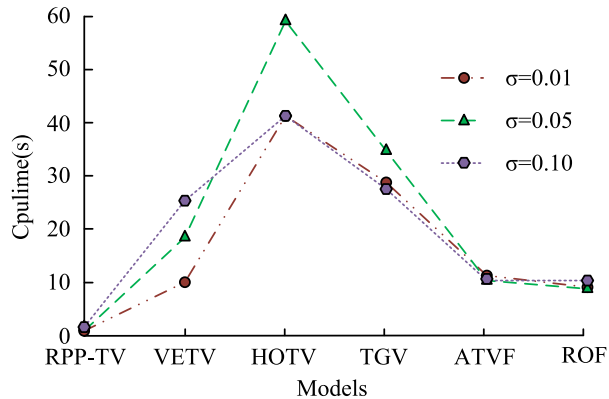
(a) Comparison of CPU running time of the
model for denoising Parrot images
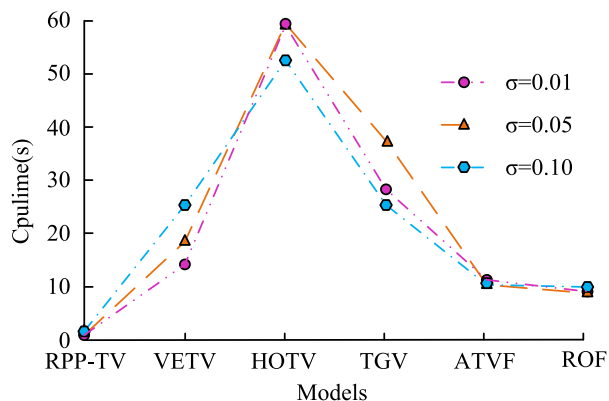


(b) Comparison of CPU running time of the
model for denoising Phantom images
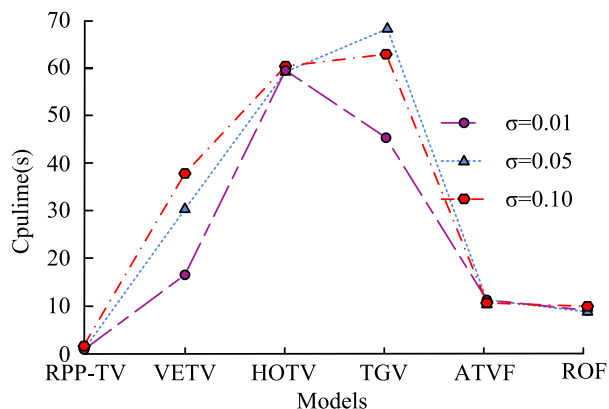


(c) Comparison of CPU running time of the
model for denoising Frame images

**FIGURE 7.** Comparison of CPU runtime for different models.

actual denoising effect. Figure 7 shows the CPU runtime of six models for denoising three images under different balance parameters.

According to Figure 7, the proposed RPP-TV denoising model had lower CPU runtime when denoising three images than other comparison models, and its CPU runtime for Par-

rot, Phantom, and Frame denoising was 0.35s, 0.78s, and 0.69s, respectively. In addition, the overall performance of the RPP-TV denoising model varied slightly when obtaining different equilibrium parameters, and its performance was the best when the equilibrium parameter was 0.01. The above results confirmed that the proposed RPP-TV denoising model had superiority over other denoising models for CPU runtime. To further evaluate the performance of the proposed denoising model, Figure 8 also shows the convergence curves of different models for re-storing noisy images.

According to Figure 8, for three different images, the six denoising models had almost the same denoising results, and the curve remained un-changed after 20 iterations. In addition, the proposed RPP-TV denoising model had a higher signal-to-noise ratio compared to other denoising models, and the highest signal-to-noise ratios of the RPP-TV denoising model when restoring Parrot, Phantom, and Frame were 20.9 db, 10.2 db, and 23.2 db, respectively. This result indicated that the proposed RPP-TV denoising model was more effective than other models in image denoising. Finally, to compare the denoising effects of the six models more intuitively, the study would denoise Parrot image using the six denoising models, and compare and analyze the denoised effect images. Figure 9 shows the effect of six denoising models on Parrot image after denoising.

According to Figure 9, the proposed RPP-TV denoising model successfully preserved details while eliminating the maximum noise, leaving only scattered small noise points. Moreover, its overall denoising effect was significantly better than the compared denoising models. This result confirmed that the proposed RPP-TV denoising model performed better than the comparison models in terms of denoising effectiveness. Based on the comparison of the above dimensions, the overall performance of the proposed RPP-TV denoising model was significantly better than the comparison model. Therefore, applying it to the image denoising process of thermal systems could effectively improve the overall performance of thermal inspection systems.

### B. ANALYSIS OF THE CONTROL EFFECT OF PID CONTROLLER INTEGRATED WITH COA

This study utilized COA to optimize the parameters of the PID controller. To analyze the performance of the optimized PID controller using this method, it was compared and analyzed with PID controllers based on Z-N equation and GA algorithm optimization. Firstly, in Figure 10, the controller parameters of the PID controller obtained by the three methods were compared.

According to Figure 10, the $K_p$, $K_i$, and $K_d$ values of the PID controller obtained from the Z-N equation were 40.13, 0.391, and 0.053, respectively. The $K_p$, $K_i$, and $K_d$ values of the PID controller optimized by GA were 21.41, 0.489, and 0.052, respectively. The $K_p$, $K_i$, and $K_d$ values of the PID controller obtained by the chaotic optimization method were 71.45, 0.256, and 0.082, respectively. After obtaining the parameters of three PID controllers, the
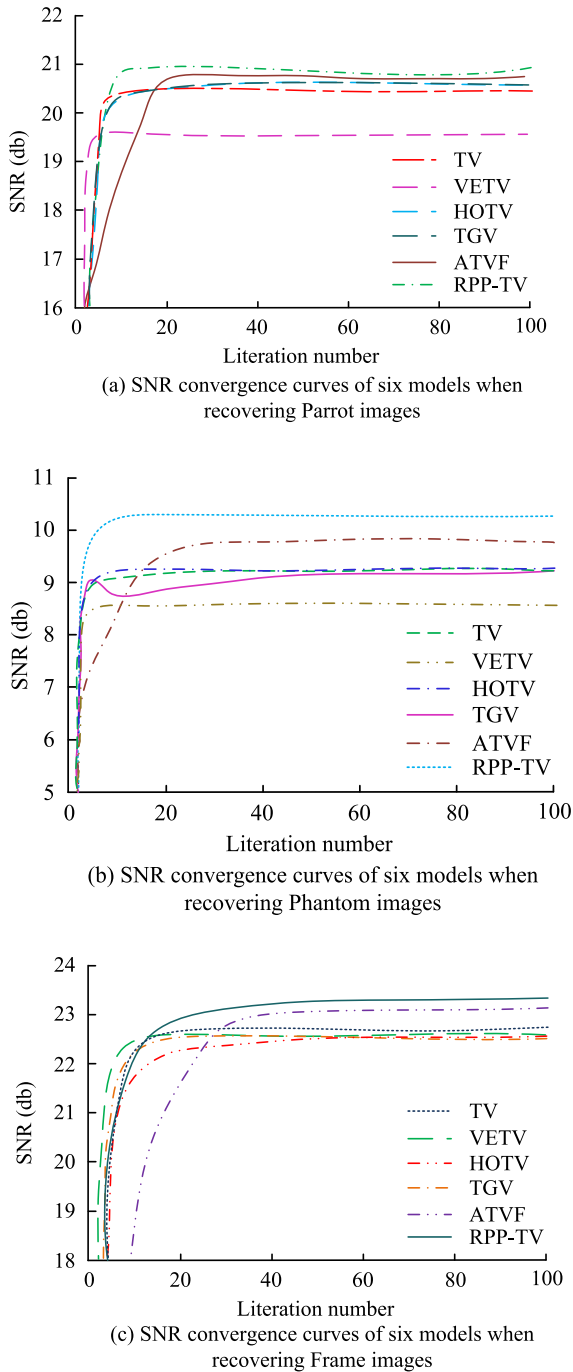
(a) SNR convergence curves of six models when recovering Parrot images



(b) SNR convergence curves of six models when recovering Phantom images



(c) SNR convergence curves of six models when recovering Frame images

**FIGURE 8.** Variation curve of SNR with the iterations.



(a) ROF



(b) VETV



(c) HOTV



(d) TGV



(e) ATVF



(f) RPP-TV

**FIGURE 9.** Effect of six denoising models on Parrot image after denoising.
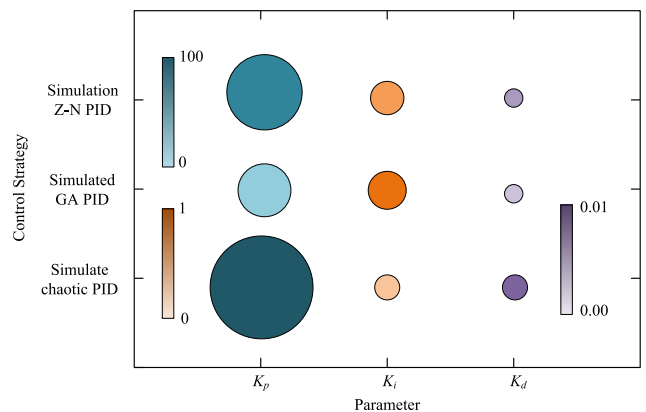


**FIGURE 10.** PID controller parameters obtained by different methods.

dynamic characteristic indicators of the unit step response under the action of the three PID controllers were calculated. Figure 11 shows the dynamic characteristics indicators of Z-N PID, GA-PID, and PID control based on chaos optimization parameter tuning.

According to Figure 11, the adjustment time, peak time, and rise time of the chaos optimized PID controller were 0.719s, 0.731s, and 0.595s, respectively. The adjustment time, peak time, and rise time of the Z-N PID controller
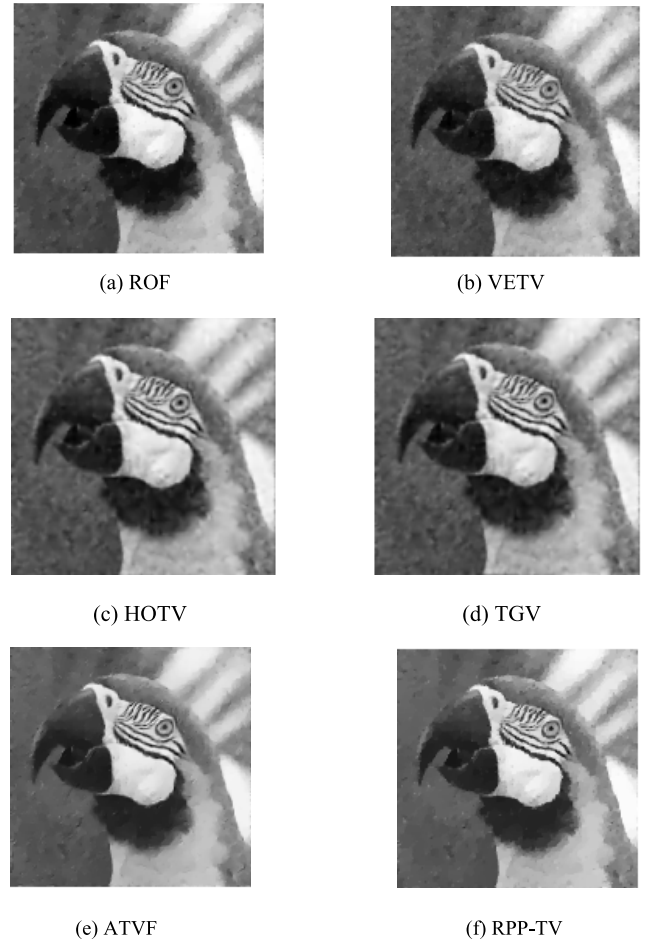
were 1.822s, 0.714s, and 0.614s, respectively. The adjustment time, peak time, and rise time of the GA-PID controller were 1.388s, 0.803s, and 0.713s, respectively. In addition, it could be analyzed from Figure 11 that the overshoot of Z-N PID controller, chaos optimized PID controller, and GA-PID controller were 21.3%, 0.53%, and 0%, respectively. The above results indicated that the PID controller based on
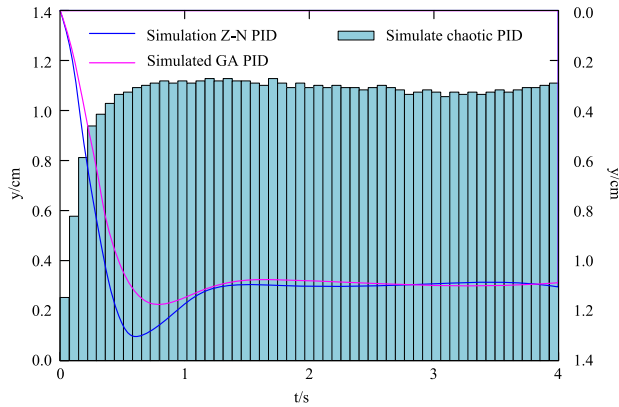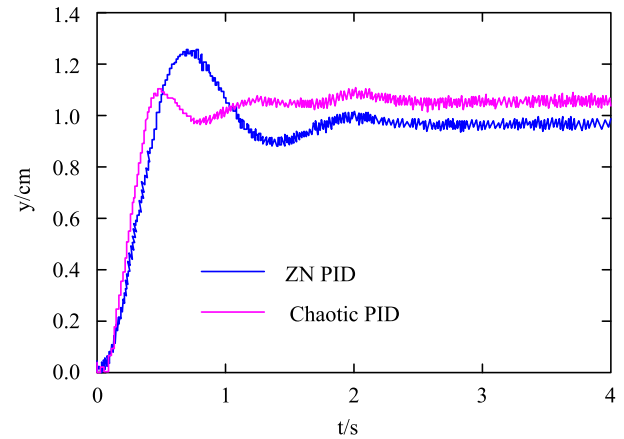
**FIGURE 11.** Comparison results of dynamic characteristic indicators of three PID controllers.



(a) Step response curve when the system pressure is 10 MPa



(b) Step response curve when the system pressure is 15 MPa

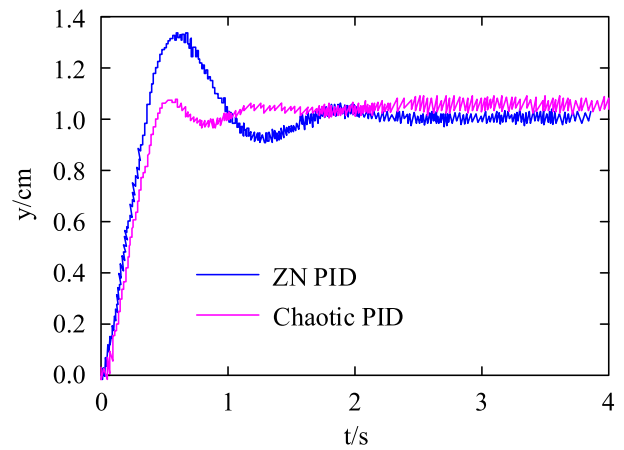**FIGURE 12.** Step response curves under two control strategies.

chaos optimization parameter tuning had better control performance than the comparison controller, with faster response speed and smaller over-shoot of the target. To further analyze the effectiveness of the chaotic PID controller, the control system pressure was adjusted to 10 MPa and 15 MPa, respectively, and step experiments were conducted under the Z-N PID controller and chaotic PID controller on the material testing machine with elastic load. Figure 12 shows the step response curves of two PID controllers.

According to Figure 12 (a), when the control system pressure was 10 MPa, the peak times of the chaos optimized PID controller and Z-N PID controller were 0.618 s and 0.832 s, respectively. And the adjustment times of the chaos optimized PID controller and Z-N PID controller were 1.121s and 1.384s, respectively. These results confirmed that under a control system pressure of 10 MPa, the control effect of the chaos optimized PID controller was better than that of Z-N PID controller. According to Figure 12 (b), when the control system pressure was 15 MPa, the peak times of the chaos optimized PID controller and Z-N PID controller were 0.703 s and 0.756 s, respectively. And the adjustment times of the chaos optimized PID controller and Z-N PID controller were 1.135s and 1.653s, respectively. This result indicated that under a control system pressure of 15 MPa, the control effect of the chaos optimized PID controller was also better than that of Z-N PID controller. Afterwards, two controllers were used for simulation in Figure 13.

According to Figure 13, the simulation and experimental curve trends of these two controllers were basically consistent, and the experimental response time was longer compared to the simulation response time under the same conditions. In addition, compared to Z-N PID controllers, chaotic optimization PID controllers achieved stability earlier. The above results indicated that the chaotic optimization PID controller had better control effect and effectiveness. Therefore, applying it to the construction of thermal inspection systems could enhance the overall performance of thermal inspection systems.
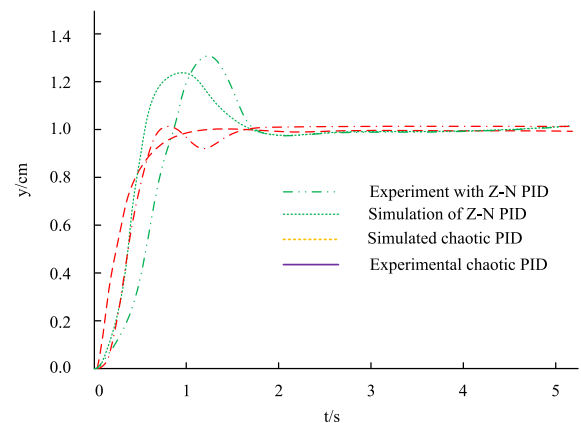


**FIGURE 13.** Simulation and experimental results of two control strategies.

## C. ANALYSIS OF THE PRACTICAL APPLICATION EFFECT OF A NEW THERMAL INSPECTION SYSTEM MODEL

After the completion of the thermal system design based on chaos optimization strategy and RPROP, it was applied in the thermal equipment inspection of a certain factory in the experiment to analyze its practical application effect. Part

(a) Standard image of thermal systems 1



(b) Standard image of thermal systems 2



(c) Standard image of thermal systems 3

**FIGURE 14.** Part of the inspection image of the thermal system.

**TABLE 1.** Detection accuracy and detection time obtained by the two inspection systems.

| / | New thermal inspection system | | Traditional thermal inspection system | |
|---|---|---|---|---|
| | Accuracy rate | Detection time | Accuracy rate | Detection time |
| 1 | 95% | 27 min | 76% | 51 min |
| 2 | 94% | 30 min | 81% | 53 min |
| 3 | 96% | 28 min | 77% | 50 min |
| 4 | 95% | 29 min | 80% | 55 min |
| 5 | 93% | 28 min | 75% | 51 min |

**TABLE 2.** Detection accuracy and detection time obtained by the two inspection systems.

| / | New thermal inspection system | | Thermal inspection system based on machine vision | |
|---|---|---|---|---|
| | Accuracy rate | Detection time | Accuracy rate | Detection time |
| 1 | 96% | 27 min | 88% | 43 min |
| 2 | 95% | 28 min | 87% | 41 min |
| 3 | 95% | 29 min | 86% | 40 min |
| 4 | 94% | 30 min | 89% | 39 min |
| 5 | 94% | 27 min | 85% | 42 min |

of the inspection image of the thermal system is shown in Figure 14.

The actual application effect of the thermal inspection system was analyzed based on its detection accuracy, detection time, and ratings from relevant personnel. This experiment would propose a new thermal inspection system and a traditional thermal inspection system to inspect 500 thermal equipment. For the convenience of statistics, the 500 thermal equipment would be evenly divided into five groups. Table 1 shows the detection accuracy and detection time obtained by two inspection systems.

According to Table 1, the overall detection accuracy of the proposed new thermal inspection system was higher than

that of traditional thermal inspection system. And the average detection accuracy of the new thermal inspection system was 94.6%, significantly better than 77.8% of the traditional thermal inspection system. In addition, the overall detection time of the proposed new thermal inspection system was lower than that of traditional thermal inspection system. And the average detection time of the new thermal inspection system was 28.4 minutes, significantly better than the 52.0 minutes of traditional thermal inspection system. Then, the new thermal inspection system proposed in this study and the thermal inspection system based on machine vision were compared and tested to demonstrate its superiority in the above experimental environment. The detection accuracy and detection time obtained by the two inspection systems are shown in Table 2.

From Table 2, the overall detection accuracy of the proposed new thermal inspection system was also higher than that of the machine vision-based thermal inspection system. Moreover, its overall detection time was also lower than that of the thermal inspection system based on machine vision. The above results demonstrated the advantages of the proposed thermal inspection system in this study compared to the more popular thermal inspection system at present. In addition, 100 relevant practitioners were selected as evaluators and randomly divided into two groups to further evaluate the practical application effect of the proposed new thermal inspection system. The performance differences between the new thermal inspection system and the traditional thermal inspection system were analyzed by comparing the reliability, effectiveness, and real-time performance ratings of two groups of evaluators. Figure 15 shows the ratings of two thermal inspection systems. The maximum score was 100 points, and a high score indicated that the indicator was good.

According to Figure 15 (a), the average scores for reliability, effectiveness, and real-time performance of the new thermal inspection system were 88.3 points, 89.7 points, and
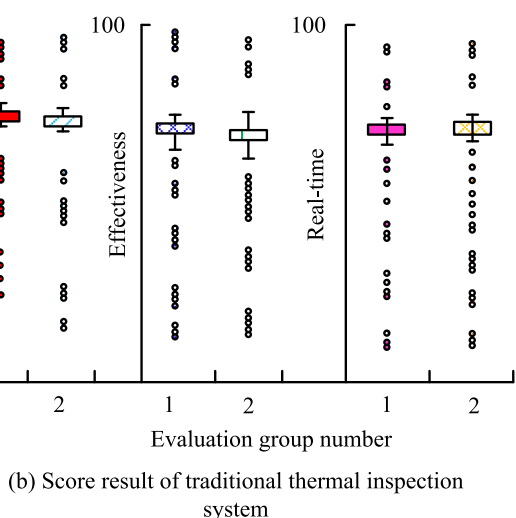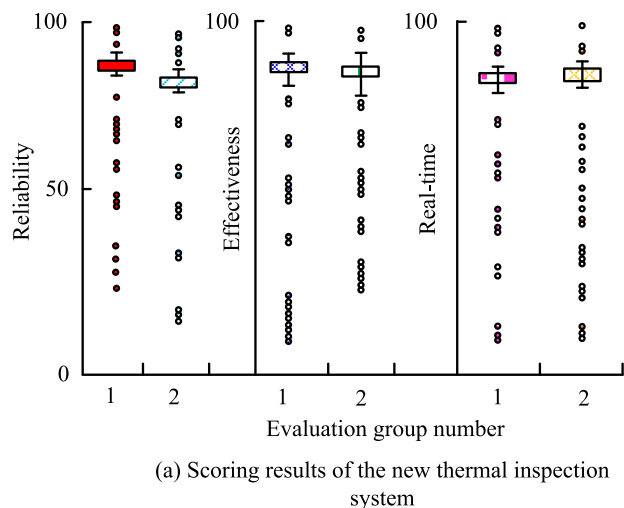
(a) Scoring results of the new thermal inspection system



(b) Score result of traditional thermal inspection system

**FIGURE 15. Scoring results of two thermal inspection systems.**

**TABLE 3. Comparison results of different thermal inspection systems.**

| Type of inspection system | Accuracy rate | Inspection time |
|---|---|---|
| The thermal inspection system proposed in this study | 94.6% | 28.4min |
| Thermal inspection system based on machine vision | 83.5% | 41.5min |
| Thermal inspection system based on machine learning | 84.2% | 36.8min |
| Thermal inspection system based on image recognition | 84.4% | 38.4min |

88.1 points, respectively. According to Figure 15 (b), the average scores for reliability, effectiveness, and real-time performance of traditional inspection system were 72.5 points, 70.3 points, and 71.8 points, respectively. Overall, relevant practitioners had a higher overall performance evaluation of

the proposed new thermal inspection system, indicating that the performance of the new thermal inspection system was better.

## V. CONCLUSION

In response to the shortcomings of incomplete equipment monitoring and inaccurate fault diagnosis in the current thermal inspection system, a new thermal inspection system was designed in this study. In the thermal inspection system, RPP-TV fused with RPROP was applied to denoise visible light images to improve image quality and thermal information accuracy. Then, a PID controller fused with COA was used to analyze and process the extracted thermal information, and corresponding alarm and diagnostic results were provided. Comparative experiments were conducted on the performance of the proposed RPP-TV denoising model and the chaos optimized PID controller. These results confirmed that the highest signal-to-noise ratios of the RPP-TV denoising model in restoring Parrot, Phantom, and Frame were 20.9db, 10.2db, and 23.2db, respectively, which were significantly better than the comparison models. The peak time and adjustment time of the chaos optimized PID controller were 0.618s and 1.121 s, respectively, which were significantly better than the 0.832 s and 1.384s of the Z-N PID controller. In the empirical analysis of the thermal inspection system, the average scores of reliability, effectiveness, and real-time performance of the new thermal inspection system were 88.3 points, 89.7 points, and 88.1 points, respectively, significantly better than the traditional inspection system's 72.5 points, 70.3 points, and 71.8 points.

In addition, the thermal inspection system proposed in this study was compared with some previous similar work, and Table 3 was obtained.

From Table 3, the accuracy and time consuming of the thermal engineering system proposed in the study were superior to the comparison systems. The above results indicated that the performance of the proposed new thermal inspection system was significantly superior to traditional inspection systems. This is thanks to the application of the RPP-TV denoising model and chaos optimized PID controller, which improves image quality and thermal information accuracy, thereby providing more accurate and timely alarm and diagnostic results. However, although this study has achieved remarkable results, there are still some shortcomings that need to be further explored. First, the RPP-TV denoising model may have limitations when dealing with specific types of noise and needs to be further optimized and improved to adapt to a wider range of application scenarios. Secondly, chaos optimized PID controller may need more refined parameter adjustment and optimization strategy in the face of complex and changeable thermal environment. To solve the above issues, future research can be conducted in the following aspects: First, more advanced denoising technologies should be explored to improve the image quality and accuracy of thermal information, such as deep learning denoising algorithm, non-local mean denoising algorithm,

BM3D algorithm and other optimized denoising algorithms. Second, the chaotic optimization PID controller is further improved to adapt to more complex and changeable thermal environment by parameter adaptive adjustment, intelligent control strategy integration, multi-mode control, etc., such as high temperature and humidity environment, rapid temperature change environment, corrosive thermal environment, radiation thermal environment, etc. The third is to consider applying artificial intelligence, machine learning, and other intelligent technologies to the thermal inspection system to achieve more intelligent and autonomous equipment monitoring and fault diagnosis functions. The fourth is to conduct more extensive empirical research to verify the applicability and stability of the new thermal inspection system in different scenarios. Through the in-depth exploration and practice of these research directions, it is expected to provide new ideas and methods for the performance improvement and intelligent development of thermal inspection systems.

## REFERENCES

[1] A. Lajunen, Y. Yang, and A. Emadi, "Review of cabin thermal management for electrified passenger vehicles," *IEEE Trans. Veh. Technol.*, vol. 69, no. 6, pp. 6025–6040, Jun. 2020, doi: 10.1109/TVT.2020.2988468.

[2] F. Shen, P. Ju, M. Shahidehpour, Z. Li, C. Wang, and X. Shi, "Singular perturbation for the dynamic modeling of integrated energy systems," *IEEE Trans. Power Syst.*, vol. 35, no. 3, pp. 1718–1728, May 2020, doi: 10.1109/TPWRS.2019.2953672.

[3] Y. Zhang, Z. Wang, H. Wang, and F. Blaabjerg, "Artificial intelligence-aided thermal model considering cross-coupling effects," *IEEE Trans. Power Electron.*, vol. 35, no. 10, pp. 9998–10002, Oct. 2020, doi: 10.1109/TPEL.2020.2980240.

[4] A. S. Maihulla, I. Yusuf, and S. I. Bala, "Reliability and performance analysis of a series-parallel system using gumbel–hougaard family copula," *J. Comput. Cognit. Eng.*, vol. 1, no. 2, pp. 74–82, Dec. 2021, doi: 10.47852/bonviewjcce2022010101.

[5] Z. Xu, H. Yang, J. Li, X. Zhang, B. Lu, and S. Gao, "Comparative study on single and multiple chaotic maps incorporated grey wolf optimization algorithms," *IEEE Access*, vol. 9, pp. 77416–77437, 2021, doi: 10.1109/ACCESS.2021.3083220.

[6] X. Yang and L. Cheng, "Hyper-spectral image pixel classification based on golden sine and chaotic spotted hyena optimization algorithm," *IEEE Access*, vol. 11, pp. 89757–89768, 2023, doi: 10.1109/ACCESS.2023.3307196.

[7] G. Chen, Z. Li, Z. Zhang, and S. Li, "An improved ACO algorithm optimized fuzzy PID controller for load frequency control in multi area interconnected power systems," *IEEE Access*, vol. 8, pp. 6429–6447, 2020, doi: 10.1109/ACCESS.2019.2960380.

[8] S. Gao, Y. Yu, Y. Wang, J. Wang, J. Cheng, and M. Zhou, "Chaotic local search-based differential evolution algorithms for optimization," *IEEE Trans. Syst. Man, Cybern. Syst.*, vol. 51, no. 6, pp. 3954–3967, Jun. 2021, doi: 10.1109/TSMC.2019.2956121.

[9] R. Yu and P. Li, "Toward resource-efficient federated learning in mobile edge computing," *IEEE Netw.*, vol. 35, no. 1, pp. 148–155, Jan. 2021, doi: 10.1109/MNET.011.2000295.

[10] C. Yan, J. Chen, H. Liu, and H. Lu, "Model-based fault tolerant control for the thermal management of PEMFC systems," *IEEE Trans. Ind. Electron.*, vol. 67, no. 4, pp. 2875–2884, Apr. 2020, doi: 10.1109/TIE.2019.2912772.

[11] Y. Duan, N. Chen, L. Chang, Y. Ni, S. V. N. S. Kumar, and P. Zhang, "CAPSO: Chaos adaptive particle swarm optimization algorithm," *IEEE Access*, vol. 10, pp. 29393–29405, 2022, doi: 10.1109/ACCESS.2022.3158666.

[12] M. Premkumar, P. Jangir, C. Ramakrishnan, G. Nalinipriya, H. H. Alhelou, and B. S. Kumar, "Identification of solar photovoltaic model parameters using an improved gradient-based optimization algorithm with chaotic drifts," *IEEE Access*, vol. 9, pp. 62347–62379, 2021, doi: 10.1109/ACCESS.2021.3073821.

[13] P. Priyadarshi and C. S. Rai, "Rprop and improved Rprop+ based constant modulus type (RCMT) blind channel equalization algorithm for QAM signal," *J. Inf. Optim. Sci.*, vol. 40, no. 2, pp. 351–366, Mar. 2019, doi: 10.1080/02522667.2019.1586351.

[14] S. A. Abdulkarim and A. P. Engelbrecht, "Time series forecasting with feedforward neural networks trained using particle swarm optimizers for dynamic environments," *Neural Comput. Appl.*, vol. 33, no. 7, pp. 2667–2683, Jul. 2020, doi: 10.1007/s00521-020-05163-4.

[15] X. Wang, H. He, and L. Li, "A hierarchical deep domain adaptation approach for fault diagnosis of power plant thermal system," *IEEE Trans. Ind. Informat.*, vol. 15, no. 9, pp. 5139–5148, Sep. 2019, doi: 10.1109/TII.2019.2899118.

[16] W. Violante, C. A. Cañizares, M. A. Trovato, and G. Forte, "An energy management system for isolated microgrids with thermal energy resources," *IEEE Trans. Smart Grid*, vol. 11, no. 4, pp. 2880–2891, Jul. 2020, doi: 10.1109/TSG.2020.2973321.

[17] J. Tóth and I. Farkas, "Predictive control of a solar thermal system via on-line communication with a meteorological database server," *Idojárás*, vol. 125, no. 2, pp. 211–227, Apr. 2021, doi: 10.28974/idojaras.2021.2.3.

[18] N. R. Babu and L. C. Saikia, "Load frequency control of a multi-area system incorporating realistic high-voltage direct current and dish-stirling solar thermal system models under deregulated scenario," *IET Renew. Power Gener.*, vol. 15, no. 5, pp. 1116–1132, Feb. 2021, doi: 10.1049/rpg2.12093.

[19] H. Shao, M. Xia, G. Han, Y. Zhang, and J. Wan, "Intelligent fault diagnosis of rotor-bearing system under varying working conditions with modified transfer convolutional neural network and thermal images," *IEEE Trans. Ind. Informat.*, vol. 17, no. 5, pp. 3488–3496, May 2021, doi: 10.1109/TII.2020.3005965.

[20] M. Ahmadi Kamarposhti, H. Shokouhandeh, M. Alipur, I. Colak, H. Zare, and K. Eguchi, "Optimal designing of fuzzy-PID controller in the load-frequency control loop of hydro-thermal power system connected to wind farm by HVDC lines," *IEEE Access*, vol. 10, pp. 63812–63822, 2022, doi: 10.1109/ACCESS.2022.3183155.

[21] T. Ding, Z. Zeng, M. Qu, J. P. S. Catalão, and M. Shahidehpour, "Two-stage chance-constrained stochastic thermal unit commitment for optimal provision of virtual inertia in wind-storage systems," *IEEE Trans. Power Syst.*, vol. 36, no. 4, pp. 3520–3530, Jul. 2021, doi: 10.1109/TPWRS.2021.3051523.

[22] S. Lu, W. Gu, K. Meng, and Z. Dong, "Economic dispatch of integrated energy systems with robust thermal comfort management," *IEEE Trans. Sustain. Energy*, vol. 12, no. 1, pp. 222–233, Jan. 2021, doi: 10.1109/TSTE.2020.2989793.

[23] A. Aryal, B. Becerik-Gerber, G. M. Lucas, and S. C. Roll, "Intelligent agents to improve thermal satisfaction by controlling personal comfort systems under different levels of automation," *IEEE Internet Things J.*, vol. 8, no. 8, pp. 7089–7100, Apr. 2021, doi: 10.1109/JIOT.2020.3038378.

[24] B. Babes, F. Albalawi, N. Hamouda, S. Kahla, and S. S. M. Ghoneim, "Fractional-fuzzy PID control approach of photovoltaic-wire feeder system (PV-WFS): Simulation and HIL-based experimental investigation," *IEEE Access*, vol. 9, pp. 159933–159954, 2021, doi: 10.1109/ACCESS.2021.3129608.

[25] M. N. Ali, M. Soliman, K. Mahmoud, J. M. Guerrero, M. Lehtonen, and M. M. F. Darwish, "Resilient design of robust multi-objectives PID controllers for automatic voltage regulators: D-Decomposition approach," *IEEE Access*, vol. 9, pp. 106589–106605, 2021, doi: 10.1109/ACCESS.2021.3100415.

[26] O. Rodríguez-Abreo, J. Rodríguez-Reséndiz, C. Fuentes-Silva, R. Hernández-Alvarado, and M. D. C. P. T. Falcón, "Self-tuning neural network PID with dynamic response control," *IEEE Access*, vol. 9, pp. 65206–65215, 2021, doi: 10.1109/ACCESS.2021.3075452.

[27] J. J. Castillo-Zamora, K. A. Camarillo-GóMez, G. I. PéRez-Soto, and J. RodríGuez-ReséNdiz, "Comparison of PD, PID and sliding-mode position controllers for V–tail quadcopter stability," *IEEE Access*, vol. 6, pp. 38086–38096, 2018, doi: 10.1109/ACCESS.2018.2851223.

[28] L.-H. Zhao, S. Wen, M. Xu, K. Shi, S. Zhu, and T. Huang, "PID control for output synchronization of multiple output coupled complex networks," *IEEE Trans. Netw. Sci. Eng.*, vol. 9, no. 3, pp. 1553–1566, May 2022, doi: 10.1109/TNSE.2022.3147786.

[29] R. Whitt, D. Huitink, A. Emon, A. Deshpande, and F. Luo, "Thermal and electrical performance in high-voltage power modules with non-metallic additively manufactured impingement coolers," *IEEE Trans. Power Electron.*, vol. 36, no. 3, pp. 3192–3199, Mar. 2021, doi: 10.1109/TPEL.2020.3015226.

**JIN QU** was born in Suiyang, Guizhou, Han Nationality, in 1976. He received the bachelor's degree in industrial automation and instrumentation from the Department of Radio Engineering, Fuzhou University, Fujian, in 1997, the master's degree in business administration from the School of Management, Guizhou University, in 2012, with a focus on power generation technology management.

From 1997 to 1998, he was a Maintenance Technician with the Flow and Pressure Team, Thermal Branch, Zunyi Power Plant. From 1998 to 2004, he was the Head of the Electrical and Thermal Quality Inspection Team and a Thermal Engineer of 300-MW units at Guizhou North Power Plant. From 2004 to 2010, he was the Director of the Maintenance Department 2 and the Biotechnology Department, Qianxi Power Plant, and the General Manager of Guizhou Qianxi Liyuan Environmental Protection Technology Development Company Ltd. From July 2010 to January 2013, he was the Senior Director of the Thermal Power, Safety and Environmental Protection Supervision Department, Guizhou Jinyuan Group Company Ltd., China Power Investment Corporation. From January 2013 to July 2017, he was the Executive Vice General Manager of Datang Guizhou Fa'er Power Generation Company Ltd. From 2017 to 2020, he was a member of the Party Committee and the Deputy General Manager of Guizhou Qianxi Zhongshui Power Generation Company Ltd. From April 2020 to September 2020, he was the Deputy Director of the Marketing Department, Guizhou Jinyuan Company Ltd., Headquarters of State Power Investment Group. From 2020 to 2021, he was the Deputy Director of the Marketing and Fuel Management Department, Guizhou Jinyuan Company Ltd. From 2021 to 2023, he was the Executive Director, the General Manager, and a Deputy Party Secretary of Guizhou Jinyuan Tea Garden Power Generation Company Ltd. Since July 2023, he has been with Spic Guizhou Jinyuan Company Ltd. He is also a Party and the Deputy General Manager. He has published two articles in core journals, such as Power Systems and Big Data, Title: "Discussion on testing of ETS emergency tripping system for steam turbines" and "Thinking on developing benchmarking fossil-fuel power station." He has a utility model patent related to a common box busbar supporting an insulating bracket and the invention patent relates to a pretreatment sampling and analyzing device and a fossil-fuel power station feeder control logic. His research interest includes computer software including power plant intelligent operation management systems based on digital twinning visualization.

**ZHILIN LI** was born in Guiyang, Guizhou, Ethnic Bai People, in 1990. He received the degree in computer science and technology from the College of Humanities and Technology, Guizhou Minzu University, in 2013.

From July 2013 to May 2015, he was with the Overhauler of the Electric Heating Maintenance Department, Guizhou Jinyuan Qianbei Power Plant. From May 2015 to August 2015, he was the Construction Manager of the Electric Heating Maintenance Department, Spic Guizhou Jinyuan Chayuan Power Company Ltd. From November 2015 to December 2015, he was a Thermal Control Class II Maintenance Employee with the Thermal Maintenance Department, Guizhou Jinyuan Chayuan Power Company Ltd. From January 2016 to January 2018, he was a Hot-Control Class 1 Hot-Control Maintenance Employee with the Electric Heating Maintenance Department, Guizhou Jinyuan Chayuan Power Company Ltd. From January 2018 to October 2019, he was a Thermal Monitor with the Thermal Maintenance Department, Guizhou Jinyuan Chayuan Power Company Ltd. From October 2019 to September 2021, he was with the Heating Department, Guizhou Jinyuan Chayuan Power Company Ltd. From September 2021 to June 2022, he was with the Thermal Engineering Department, Guizhou Jinyuan Chayuan Power Company Ltd. From June 2022 to August 2023, he was the Deputy Director (Chair) with the Electric Heating Maintenance Department, Guizhou Jinyuan Chayuan Power Company Ltd. Since 2023, he has been the Director of the Electric Heating Maintenance Department, Spic Guizhou Jinyuan Chayuan Power Company Ltd. He has a utility model patent relates to material level detection device. He has published papers in "Power Plant DCS Problems and Solutions Analysis."

○ ○ ○